

MedChemComm

Accepted Manuscript

This article can be cited before page numbers have been issued, to do this please use: J. Low, M. Bartberger, K. Chen, Y. Cheng, M. Fielden, V. Gore, D. Hickman, Q. Liu, A. Sickmier, H. VArgas, J. Werner, R. White, D. Whittington, S. Wood and A. E. Minatti, *Med. Chem. Commun.*, 2017, DOI: 10.1039/C7MD00106A.



This is an Accepted Manuscript, which has been through the Royal Society of Chemistry peer review process and has been accepted for publication.

Accepted Manuscripts are published online shortly after acceptance, before technical editing, formatting and proof reading. Using this free service, authors can make their results available to the community, in citable form, before we publish the edited article. We will replace this Accepted Manuscript with the edited and formatted Advance Article as soon as it is available.

You can find more information about Accepted Manuscripts in the [author guidelines](#).

Please note that technical editing may introduce minor changes to the text and/or graphics, which may alter content. The journal's standard [Terms & Conditions](#) and the ethical guidelines, outlined in our [author and reviewer resource centre](#), still apply. In no event shall the Royal Society of Chemistry be held responsible for any errors or omissions in this Accepted Manuscript or any consequences arising from the use of any information it contains.



ARTICLE

Development of 2-Aminooxazoline 3-Azaxanthene β -Amyloid Cleaving Enzyme (BACE) Inhibitors with Improved Selectivity against Cathepsin D[†]

Received 00th January 20xx,
Accepted 00th January 20xx

DOI: 10.1039/x0xx00000x

www.rsc.org/

Jonathan D. Low,^a Michael D. Bartberger,^b Kui Chen,^c Yuan Cheng,^a Mark R. Fielden,^d Vijay Gore,^{†a} Dean Hickman,^e Qingyan Liu,^a E. Allen Sickmier,^f Hugo M. Vargas,^d Jonathan Werner,^d Ryan D. White,^g Douglas A. Whittington,^f Stephen Wood,^h Ana E. Minatti,^{*a}

As part of an ongoing effort at Amgen to develop a disease-modifying therapy for Alzheimer's disease, we have previously used the aminooxazoline xanthene (AOX) scaffold to generate potent and orally efficacious BACE1 inhibitors. While AOX-BACE1 inhibitors demonstrated acceptable cardiovascular safety margins, a retinal pathological finding in rat toxicological studies demanded further investigation. It has been widely postulated that such retinal toxicity might be related to off-target inhibition of Cathepsin D (CatD), a closely related aspartyl protease. We report the development of AOX-BACE1 inhibitors with improved selectivity against CatD by following a structure- and property-based approach. Our efforts culminated in the discovery of a picolinamide-substituted 3-aza-AOX-BACE1 inhibitor absent of retinal effects in an early screening rat toxicology study.

Introduction

A widely held hypothesis for the underlying pathogenesis of Alzheimer's disease (AD) proposes aggregation of β -amyloid peptides (A β) and cerebral deposition of amyloid plaques as critical events.¹ A β is produced via sequential endoproteolytic cleavage of amyloid precursor protein (APP) by the aspartyl protease β -site APP cleaving enzyme-1 (BACE1) and γ -secretase.² Inhibition of BACE1 decreases production of all major forms of A β including the most pathogenic species A β ₄₂, suggesting that BACE1 is a prime therapeutic target for the development of disease modifying therapies for AD.³⁻⁶ The

translation of changes in cerebrospinal fluid A β levels, as an effect biomarker for brain A β lowering, in response to small molecule BACE1 inhibition is well established in rodents and higher preclinical animal species.⁷ The first prominent and long-lasting A β reduction in human lumbar cerebrospinal fluid (CSF) was disclosed in 2011.⁸ Since then, several companies have advanced additional small molecule BACE1 inhibitors to human clinical trials for the treatment of AD.⁹⁻¹¹ Potential safety liabilities of BACE1 inhibitors are less well studied. As an example, the development of the clinical candidate LY2811376 was terminated in phase 1 due to adverse retinal toxicity in a 3-month rat preclinical toxicology study.⁸ We reported a similar pathology in a 1-month preclinical toxicology study in Sprague Dawley rats administered with the lead compound, AMG-8718.^{12,13} Retinal toxicity in the rat was characterized by retinal thinning preceded by the accumulation of autofluorescent granules (AFG) in the retinal pigment epithelium (RPE), suggestive of disruption of phagolysosomal function in the RPE.¹⁴ These findings prompted us and others to evaluate additional BACE1 inhibitors for their potential to increase AFG in the RPE of preclinical species, as an early marker of incipient retinal thinning. To date, the results of several preclinical toxicology studies involving BACE1 inhibitors as they relate to retinal toxicity have been disclosed (Figure 1): six BACE1 inhibitors tested "positive" for induction of AFG in the RPE (LY2811376,⁸ AMG-8718^{12,13}, 1¹⁵, PF-3195,¹⁶ PF-1283,¹⁶ and PF-9283¹⁶) whereas four BACE1 inhibitors tested "negative" (LY2886721,^{16,17} 2,¹⁸ 3,¹⁶ and NB-360¹⁹). We report herein the discovery of an aminooxazoline xanthene (AOX)-BACE1 inhibitor (Figure 1, 30) that is devoid of early signs of retinal pathology.

^a Department of Medicinal Chemistry, Amgen Inc., One Amgen Center Drive, Thousand Oaks, CA 91320, USA.

^b Department of Molecular Engineering, Amgen Inc., One Amgen Center Drive, Thousand Oaks, CA 91320, USA.

^c Department Discovery Technologies, Amgen Inc., One Amgen Center Drive, Thousand Oaks, CA 91320, USA.

^d Comparative Biology and Safety Sciences, Amgen Inc., One Amgen Center Drive, Thousand Oaks, CA 91320, USA.

^e Department of Pharmacokinetics and Drug Metabolism, Amgen Inc., One Amgen Center Drive, Thousand Oaks, CA 91320, USA.

^f Department of Molecular Engineering, Amgen Inc., 360 Binney Street, Cambridge, MA 02142, USA.

^g Department of Medicinal Chemistry, Amgen Inc., 360 Binney Street, Cambridge, MA 02142, USA.

^h Department of Neuroscience, Amgen Inc., One Amgen Center Drive, Thousand Oaks, CA 91320, USA.

* Corresponding author: aminatti@amgen.com; +1 805 447 4721

[†] Present Address: Knobbe Martens Intellectual Property Law, 2040 Main Street, 14th Floor, Irvine, CA 92614.

‡The authors declare no competing interests.

Electronic Supplementary Information (ESI) available: [details of any supplementary information available should be included here]. See DOI: 10.1039/x0xx00000x

A current hypothesis is that the retinal toxicity in preclinical species is due to off-target inhibition of Cathepsin D (CatD), a structurally related aspartyl protease that plays an important role in phagolysosomal processing in the RPE.²⁰ The scientific evidence for CatD as a possible mediator of the retinal toxicity is mounting as progress has been made linking the observed in vivo accumulation of AFG in the RPE to enzymatic (biophysical or biochemical) and cellular CatD inhibition, together with lysosomal accumulation.¹⁶

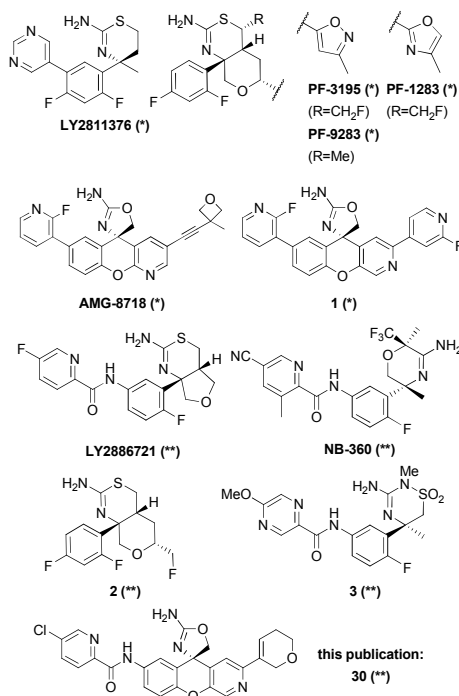


Fig 1. BACE1 inhibitors that tested “positive” (*) or “negative” (**) for induction of AFG in the RPE in preclinical species. Each study design varied with respect to preclinical species, compound dose and study length.

Our objective was to improve the selectivity of the AOX-BACE1 inhibitors against human CatD (CatD/BACE1 selectivity) by using a structure- and property-based approach. Our measurement of CatD/BACE1 selectivity was based on an enzymatic in vitro assay and we aimed for a large in vitro selectivity window.²¹ This in vitro data allowed us to quickly rank-order compounds for subsequent in vivo toxicological profiling in rats with an emphasis on retinal evaluation. We focused our efforts on the aminooxazoline 3-aza-xanthene (3-aza-AOX) core as the retinal toxicity profile of the lead molecule of this series, (compound **1** in Figure 1) had been extensively studied in rats and cynomolgus monkeys.¹⁵ Our structure-based approach was based on exploiting the residue differences in the S3 sub-pocket (S3_{sp}) – also referred to as the deep S3 pocket – of the BACE1 protein versus the CatD protein.^{18, 22} Figure 2a shows the co-crystal structure of rat CatD with BACE1 inhibitor **4**²³ (PDB 5UX4) – a closely related analog of **1**. The amino acid sequence of rat CatD shows 83 % identity with human CatD and the residues within

5Å of the co-crystallized ligand **4** are identical between the two species.^{24, 25} To the best of our knowledge, this constitutes the first time a co-crystal of a BACE1 inhibitor with the CatD protein has been published. The catalytic aspartic acids and the flap tyrosine are conserved in both CatD (Figure 2a) and BACE1 (Figure 2b, PDB 4WTU)²³ and drive the same alignment of AOX core in both proteins. The P3²⁶ group occupies the S3 pocket in CatD as well as in BACE1, but the protein surfaces reveal an opportunity to extend a vector from the 7 position of the xanthene core deeper into the S3 pocket of BACE1 and potentially increase selectivity over CatD (Figure 2 a and b). In particular, analysis of the aligned S3 regions of BACE1 and CatD (Figure 2c) reveal a key difference between an alanine residue (Ala335) in BACE1 and the correspondingly larger and more polar Asp318 residue in the same binding side region of CatD. This key steric and polar residue mismatch in a relatively buried region of the S3 subsite afforded an attractive and compelling potential selectivity handle to pursue.

The challenge was multifaceted regarding the property-based approach. The importance of choosing an amidine-type BACE1 inhibitor warhead with an optimal pK_a has been extensively discussed in the context of: a) BACE1 cell potency;²⁷⁻³⁰ b) central nervous system (CNS) exposure and robust CNS pharmacodynamic (PD) activity;^{31, 32} and c) potential lysosomal accumulation and polypharmacology.^{14, 33-35} The pK_a of the aminooxazoline warhead is influenced by the core,³¹ with the 3-aza-xanthene core maintaining the pK_a of the 2-aminooxazoline (e.g. **1** pK_a = 5.7) in a desirable range (5.5 < pK_a < 7.5); i.e., maximizing engagement with the catalytic aspartate residues within the BACE1 protein while minimizing the potential for lysosomal accumulation. Additionally, the overall properties of the molecule as they relate to CNS penetration/CNS drug-like space were closely monitored throughout the process of modifying the structure towards the goal of increasing selectivity over CatD.³⁶⁻³⁸

The aim of this work was to evaluate alkynylpyridines³⁹⁻⁴⁷ and picolinamides^{17, 19, 31, 32, 41, 46, 48-53} as P3 sub-pocket (P3_{sp}) groups on the 3-aza-AOX core and test their influence on CatD selectivity. The strategy was to initially omit the P2' substituent, in order to offset the increase in molecular weight (MW) upon extending into the S3_{sp} and maximize lipophilic efficiency (Figure 3).

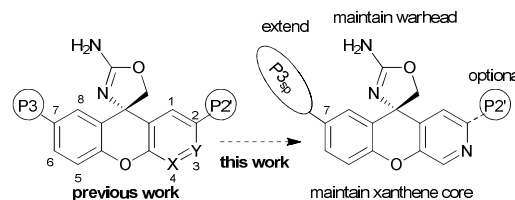


Fig 3. Strategy to improve selectivity of 3-aza-AOX-BACE1 inhibitors against CatD.

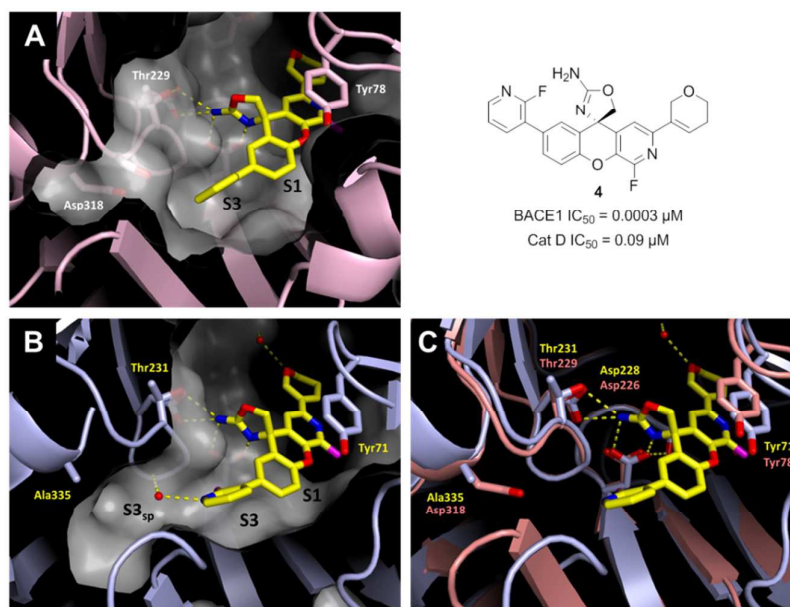
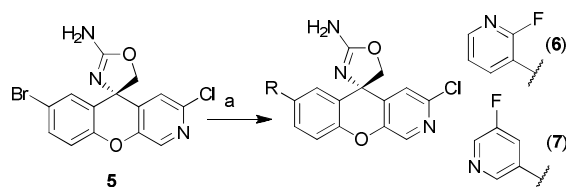


Fig 2. (a) Co-crystal structure of rat CatD and AOX-BACE1 inhibitor **4** (yellow, PDB 5UX4). The mobile flap region is shown in pink and its surface is not depicted for clarity. (b) Co-crystal structure of human BACE1 and AOX-BACE1 inhibitor **4** (yellow; PDB 4WTU).²³ Red spheres represent water molecules. The mobile flap region is shown in blue and its surface is not depicted for clarity. (c) Overlaid co-crystal structure of human BACE1 (blue) + compound **4** (yellow) overlaid with co-crystal structure of rat CatD (pink) + compound **4**. Key residues are labelled in yellow for BACE1 and pink for CatD. Key hydrogen bonds are depicted as yellow dashed lines.

Results and Discussion

Chemistry

The 3-aza-AOX BACE1 inhibitors profiled in Tables 1-3 were synthesized via several routes. The synthesis of the truncated BACE1 inhibitors **6** and **7** is shown in Scheme 1. The sequence for the synthesis of key intermediate **5** was disclosed in a previous publication¹⁵ and additional experimental details for each step including characterization of the intermediates can be found in the supporting information of this publication. Suzuki-Miyaura-coupling of the unprotected enantiomerically pure intermediate **5** with either 2-fluoro-3-pyridine boronic acid or 5-fluoro-3-pyridine boronic acid yielded compounds **6** and **7**, respectively. The reaction proceeded with high regioselectivity for the bromide (96% (**6**) and 58% (**7**) respectively) using $(Pd(AmPhos)_2Cl_2)$.⁵⁴



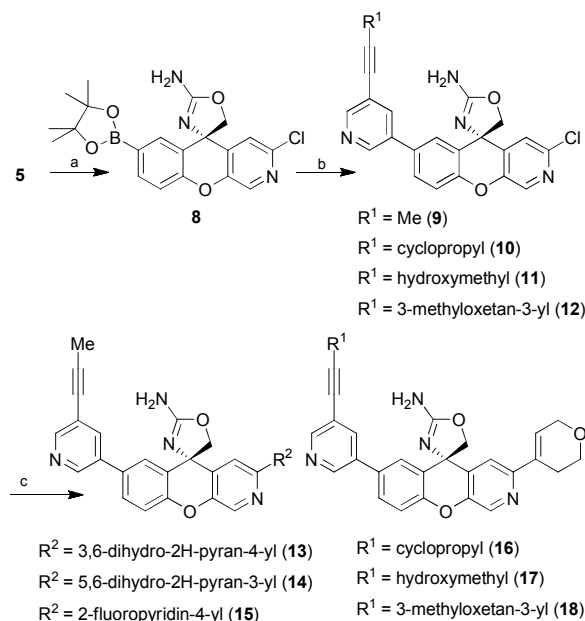
Scheme 1 Reagents: (a) 2-fluoropyridin-3-ylboronic acid or 5-fluoropyridin-3-ylboronic acid, $Pd(AmPhos)_2Cl_2$ (cat.), K_3PO_4 , dioxane/water, 100 °C, 96% (**6**) or 58% (**7**)

The synthesis of deep-P3²⁶ alkyne containing 3-aza-AOX compounds is illustrated in Scheme 2.⁵⁵ Miyaura borylation of intermediate **5** under standard reaction conditions afforded boronic ester **8** in 91% yield. Subsequent palladium-catalyzed Suzuki-cross coupling of **8** with the corresponding 3-bromo-5-alkyne-pyridines using $Pd(AmPhos)_2Cl_2$ provided compounds **9-12** in moderate yields. The chloro-pyridine of these alkyne-substituted 3-aza-AOX analogs (**9-12**) was further converted into more elaborate P2' substituents via Suzuki-cross coupling. Three privileged P2' substituents from formerly published lead AOX-BACE1 inhibitors^{15, 23, 56} were installed by using either the corresponding boronic acid or pinacol boronic ester affording compounds **13-18**.

All deep-P3 amide-substituted 3-aza-AOX compounds were synthesized via amide coupling of the corresponding amino-(phenyl)-substituted 3-aza-AOX intermediates (**20, 23-26** and **31**) and 5-chloropicolinic acid but with slight variations, as depicted in Scheme 3. For ease of discussion "protected" and "unprotected" refers to the aminooxazoline warhead functional group. Intermediate **5** was mono-benzoyl protected to give bromide **19**, which was converted to the amino-substituted-benzoyl-protected 3-aza-AOX **20** via Pd-catalyzed coupling with LiHMDS as the ammonia surrogate.⁵⁷ Intermediate **20** was reacted with 5-chloropicolinic acid under 1-ethyl-3-(3-dimethylaminopropyl)carbodiimide (EDCI) amide coupling conditions, followed by cleavage of the benzoyl protecting group using sodium hydroxide, to yield the final compound **21**.

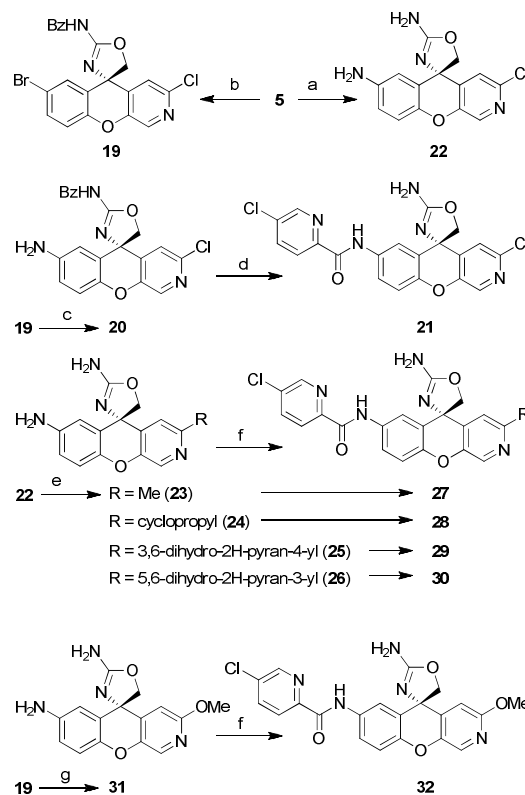
ARTICLE

MedChemComm



Scheme 2 Reagents: (a) B_2Pin_2 , $Pd(dppf)Cl_2$ (cat.), KOAc, dioxane, 91%; (b) 3-bromo-5-alkyne-pyridines, $Pd(AMPhos)_2Cl_2$ (cat.), K_3PO_4 , dioxane/water, 100 °C, 26-58%; (c) 2-(5,6-dihydro-2H-pyran-3-yl)-4,4,5,5-tetramethyl-1,3,2-dioxaborolane (for **13**, **16**, **17** and **18**), 2-(3,6-dihydro-2H-pyran-4-yl)-4,4,5,5-tetramethyl-1,3,2-dioxaborolane (for **14**), or (2-fluoropyridin-4-yl)boronic acid (for **15**) with catalyst system A ($Pd(PPh_3)_4$ (cat.), K_2CO_3 , dioxane/water, 120 °C for synthesis of **13** and **15**) or catalyst system B ($Pd(AMPhos)_2Cl_2$ (cat.), K_3PO_4 , dioxane/water, 100 °C for synthesis of **14**, **16**-**18**).

Alternatively, the unprotected amino-substituted 3-aza-AOX **22** was obtained from the unprotected bromide **5** via a Cu-catalyzed azide coupling, followed by reduction with sodium borohydride.⁵⁸ Precursor **22** was elaborated to intermediates **23-26** through Suzuki coupling without any additional protecting of either the warhead or the aminophenyl group. 4-(4,6-Dimethoxy-1,3,5-triazin-2-yl)-4-methylmorpholinium chloride (DMTMM)^{59, 60} promoted the coupling of 5-chloropicolinic acid with intermediates **23-26** giving compounds **27-30**. Analog **32** was synthesized by nucleophilic aromatic substitution of chloro-pyridine **19** with sodium methoxide, introduction of an amino-group via LiHMDS coupling, warhead deprotection, and amide coupling with 5-chloropicolinic acid.



Scheme 3 Reagents: (a) (i) NaN_3 , CuI (cat.), *trans*-N,N'-dimethylcyclohexane-1,2-diamine, sodium ascorbate, EtOH/water, 90 °C, (ii) $NaBH_4$, 80%; (b) benzoic anhydride, 90%; (c) $Pd_2(dba)_3$ (cat.), CyJohnPhos, LiHMDS, 69%; (d) (i) EDCl, HOBT, 5-chloropicolinic acid; (ii) NaOH; 36% overall yield. (e) trimethyl borate (for **23**), cyclopropyl boronic acid (for **24**) or corresponding pinacol boranes (for **25** and **26**), $Pd(AMPhos)_2Cl_2$ (cat.), K_3PO_4 , dioxane/water, 110 °C, 69-99%; (f) 5-chloropicolinic acid, DMTMM, 26-65%. (g) (i) NaOMe, 55%; (ii) $Pd_2(dba)_3$ (cat.), CyJohnPhos, LiHMDS, 71%; (iii) NaOH, 90%;

Biological Activity

As previously discussed, our strategy was to initially minimize MW by reducing the size of the P2'-substituent on the 3-aza-AOX core while fully exploiting CatD and BACE1 protein residue differences in the S3 sub-pocket. To this end P2'-Cl-substituted compound **6**, a truncated version of compound **1**, was chosen as a reference compound to monitor progress (Table 1). Despite replacing the 2-fluoro-4-pyridinyl substituent with a chlorine, compound **6** retained high potency in the BACE1 enzymatic assay (IC_{50} = 72 nM) and moderate potency in the cell assay (IC_{50} = 830 nM). The cellular potency of the compounds was assessed by measuring the inhibition of $A\beta_{40}$ production in HEK293 cells expressing APP. The CatD/BACE1 selectivity of **6** was calculated to be 210x based on measured enzymatic CatD potency. Based on the co-crystal structures shown in Figure 2a, the P3 group (2-fluoropyridin-3-yl) in **6** was replaced by a structural isomer. It was predicted that a 5-fluoro-3-pyridyl P3 group would position the fluorine in a trajectory towards the S3 sub-pocket. The affinity of the 5-fluoro-3-pyridyl analog **7** towards CatD decreased by 8.5x-fold compared to compound **6**, while the affinity towards BACE1 dropped only by 4.5x-fold (Table 1). This result suggested that

the fluorine in 5-fluoro-3-pyridyl was a potential vector into the S3 sub-pocket which could be further exploited. As a follow-up, a 5-propynyl-3-pyridyl analog **9** was prepared to further probe this vector.^{39, 40} Compound **9** showed improved BACE1 enzyme (13 nM) and cell potency (120 nM), as well as increased CatD/BACE1 selectivity (~5,600x). Additionally, the physicochemical properties of **9** were in an acceptable range for CNS penetration (MW = 402 g/mol, clogP = 3.0, PSA = 83 Å²).³⁶

Table 1 Different trajectories to access the S3 sub-pocket

Cmd #	R ¹ =				
	R ² =				
BACE1 IC ₅₀ [μM] ^a	0.00092	0.072	0.32	0.013	0.021
CatD IC ₅₀ [μM] ^a	0.66	15	130	72	1,100
HEK IC ₅₀ [μM] ^b	0.021	0.83	4.7	0.12	0.19
Selectivity^c CatD/BACE1	660	210	400	5,600	53,000
MW [g/mol]	443	383	383	402	442
clogP^d/LipE^e	2.6/6.5	2.5/4.7	2.5/4.0	3.0/4.9	2.8/4.9
PSA [Å²]/#HBD	95/1	83/1	83/1	83/1	112/2

^aIC₅₀ values were averaged values determined by at least two independent experiments. ^bHuman embryonic kidney cells. ^cSelectivity ratio [IC₅₀ CatD/IC₅₀ BACE1]. ^dclogP values were calculated using ACD LogD Suite (version 10). ^eLipE = -log₁₀(BACE1 IC₅₀) - cLogP.

As an alternative approach, we replaced the 5-substituted-3-pyridyl P3 group with an elongated picolinamide, which has been a privileged moiety heavily utilized in several previously disclosed BACE1 inhibitor designs and initially described by Shionogi.^{17, 19, 31, 32, 41, 46, 48-52} The 5-chloropicolinamide was well tolerated on the 3-aza-AOX core with compound **21** showing high enzymatic BACE1 activity (21 nM), a 10x cell shift (190 nM) and very high CatD/BACE1 selectivity (~53,000x). Of particular note, the absolute CatD IC₅₀ value exceeded 1 mM.⁶¹ The superior CatD/BACE1 selectivity obtained with the 5-chloropicolinamide-substituted compound **21** (Table 1) came at the cost of increased MW, PSA (442 g/mol, and 112 Å², respectively) and the addition of another hydrogen bond donor. In order to assess if CNS penetration, and ultimately in vivo Aβ₄₀ lowering was attainable for these 3-aza-AOX BACE1 inhibitors, data on permeability, P-gp transporter recognition and microsomal stability was collected. The results shown in Table 2 (entry 1, **9**) and Table 3 (entry 1, **21**) confirmed that both compounds were highly permeable, had low efflux ratios and low turnover in human and rat liver microsomes. These results warranted further work on both types of deep P3 groups with the goal of improving BACE1 potency without eroding selectivity towards CatD.

We replaced the chlorine in compound **9** with P2' substituents that were successfully used in former lead AOX-BACE1 inhibitors.^{15, 23, 56} Three alkyne analogs **13-15** with these privileged P2' substituents were tested in the BACE1 enzymatic and cellular assays and showed picomolar BACE1 affinity with low cell shift (Table 2). High passive permeability and low P-gp efflux ratios were maintained for all three analogs. Compound **15** was metabolically stable in rat and human liver microsomal studies, whereas increased microsomal turnover was observed for the dihydropyrans **13** and **14**. Importantly, high CatD/BACE1 selectivity was maintained for all three compounds, with the 5,6-dihydro-2H-pyran-3-yl analog **13** displaying the highest CatD/BACE1 selectivity (~19,000x). A x-ray co-crystal structure of compound **13** bound to BACE1 was obtained to confirm the hypothesized orientation of the propyne into the S3 sub-pocket (Fig. 4, PDB 5UYU). As observed in previously reported AOX-BACE1 x-ray co-crystal structure, the aminooxazoline moiety interacts with the two catalytic aspartic acids (Asp228, Asp32) and Tyr 71 engages in the π-stacking interaction with the 3-aza-AOX core. The nitrogen of the 3-aza-AOX core nitrogen forms a hydrogen bond interaction with Trp 76 through a water bridge and the dihydropyran unit resides in the S2' pocket of the protein where the oxygen atom is within hydrogen bond distance to Arg128. As proposed, the propynyl group occupies the S3 sub-pocket and engages in a lipophilic interaction with Ala335. The high CatD selectivity could be attributed to the residue difference in the S3 sub-pocket as highlighted in the CatD protein overlay in Figure 4b (Ala335 in BACE1 vs. Asp318 in CatD): whereas the methyl terminus of the propynyl moiety engages in a van der Waals interaction (3.8 Å) with the methyl group of Ala335; structural alignment of the CatD protein clearly demonstrates the repulsive steric interaction which would ensue with the Asp318 side chain of CatD.

Additional alkyne analogs (Table 2, **16-18**) were investigated in an attempt to improve the microsomal stability of **13** and explore the impact on CatD/BACE1 selectivity. A larger cell shift and moderate CatD/BACE1 selectivity was observed for the cyclopropylethynyl analog **16** and the 3-methyl-3-oxetan-ethynyl analog **18**. In addition, the hydroxymethyl analog **17** demonstrated high P-gp mediated efflux. An attempt to mask the hydroxy group in form of a 3-methyl-oxetan-3-yl group (**18**) resulted in reduced P-gp efflux.¹³ However, all three analogs **16-18** suffered from high in vitro metabolism.

We continued our investigation on the deep-P3 amide-substituted compound **21** in order to improve cell potency (Table 1 and 3). Cognizant of the physicochemical properties, small substituents were chosen as alternative P2' groups (Table 3, **27, 28** and **32**). The methoxy (**32**) and the cyclopropyl (**28**) P2' groups not only improved BACE1 enzyme and cell potency (52 nM and 13 nM, respectively) but also maintained the high CatD/BACE1 selectivity relative to chloro analog **21**. Both compounds were highly permeable with favourable P-gp efflux ratios and were stable in human and rat liver microsomes. Replacement of the chlorine by a methyl group (**27**) increased P-gp efflux ratios. To further test the limits of the CNS drug-like space as it relates to the deep-P3 amide-

ARTICLE

MedChemComm

substituted 3-aza-AOX scaffold, the occupancy of S2' pocket was maximized via implementation of dihydropyran P2' substituents (Table 3, **29** and **30**). The additional contact with the BACE1 protein due to the P2' substituents led to BACE1 affinities in the picomolar range. A low cell shift (2–4 fold) was maintained and CatD selectivity values were extremely high, ranging from ~770,000x to ~1,800,000x. Despite the high

molecular weight (MW = 490 g/mol for **29** and **30**), both analogs remained highly permeable. The increase in PSA (121 Å² for **29** and **30**) led only in the case of compound **29** to increased recognition by P-gp efflux transporter (h/rER = 6.5/8.5). Elevated turnover in microsomes was measured for both dihydropyran analogs **29** and **30**.

Table 2 P2' SAR of deep-P3 alkyne substituted 3-aza-AOX BACE1 inhibitors

Cpd	R ¹	R ²	IC ₅₀ [μM] ^a			Selectivity ^c	Papp ^d [nm/s]	P-gp efflux Ratio ^e		Microsomal stability Cl _{int} ^f [(μL/min)/mg]	
			BACE1	HEK ^b	CatD			rER	hER	RLM	HLM
9	Me		0.013	0.12	72	5,600	22	1.7	2.8	21	27
13	Me		0.00031	0.0012	5.9	19,000	18	2.1	3.1	63	77
14	Me		0.00046	0.0022	2.7	5,900	19	1.6	1.9	45	76
15	Me		0.00043	0.0041	4.5	10,000	15	1.8	2.4	20	40
16			0.0018	0.087	3.6	2,100	13	1.4	2.3	23	80
17			0.00058	0.0024	4.4	7,500	15	44	50	46	84
18			0.0055	0.10	12	2,200	18	-	5.6	73	420

^aIC₅₀ values were averaged values determined by at least two independent experiments. ^bHuman embryonic kidney cells. ^cselectivity ratio [IC₅₀ CatD/IC₅₀ BACE1].

^dApparent permeability measured in parental LLC-PK1 cells. Values are an average of apical to basolateral (A to B) and basolateral to apical (B to A) velocities and are reported as nm/s. ^eEfflux measured in LLC-PK1 cells transfected with human MDR1 and are reported as a ratio of (B to A)/(A to B). ^fRat liver microsomal (RLM) and human liver microsomal (HLM) clearance reported as apparent intrinsic clearance with no correction for binding and not scaled. Compound concentration = 1 μM. Microsomal protein concentration = 0.25 mg/mL.

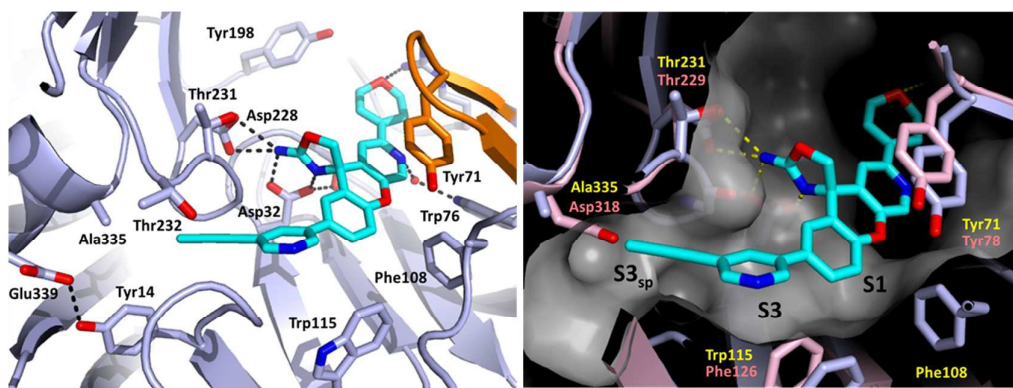


Fig 4. (a) Co-crystal structure of human BACE1 + compound **13** (turquoise, PDB 5UYU). The mobile flap region is shown in orange. Key hydrogen bonds are depicted as black dashed lines. (b) Co-crystal structure of human BACE1 (blue) + compound **13** (turquoise) overlaid with rat catD (pink). Key residues are labelled in yellow for BACE1 and pink for CatD.


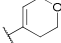
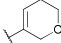
On the basis of the overall in vitro profiles and lipophilic efficiency (LipE) values (Table 3), the PD response of compounds **28**, **29** and **30** was assessed. Naïve Sprague Dawley

(SD) rats were administered a single low oral dose (10 mg/kg) of the corresponding test compound and the Aβ₄₀ levels in CSF and brain as well as exposure levels in plasma and CSF were

measured after 4 h (Table 4). While all three compounds showed comparable reduction (> 58%) of A β ₄₀ in the CSF compartment after a 10 mg/kg single oral dose, various degrees of A β ₄₀ reduction in the brain were obtained. The compounds were rank-ordered using estimated unbound plasma concentration to achieve 50% A β ₄₀ lowering in the brain from the single-point experiment.⁶² The estimated unbound plasma drug concentration corresponding to 50% A β ₄₀ reduction in the brain (EC_{50,unbound}) for compound **29** was 12-fold shifted relative to the cell IC₅₀ consistent with the previous observation that BACE1 inhibitors with large efflux ratios require higher unbound plasma concentrations relative

to IC₅₀ values to generate robust A β ₄₀ reduction.¹⁵ Compound **30** had the lowest estimated unbound plasma drug concentration corresponding to 50% A β ₄₀ reduction in the CSF (EC_{50,unbound} = 5 nM) and in the brain (EC_{50,unbound} = 11 nM) and was subsequently evaluated in a time-course PD study in rats (Figure 5). A β ₄₀ levels in the CSF and brain as well as drug plasma levels were measured at multiple timepoints in the same study. The A β ₄₀ reduction in the CSF and brain compartments of rats after a single 30 mg/kg oral dose reached its maximum after 4 hours and returned to baseline after 24 h.

Table 3 P2' SAR of deep-P3 picolinamide substituted 3-aza-AOX BACE1 inhibitors

Cpd	R	IC ₅₀ [μM] ^a			Selectivity ^c CatD/ BACE1	Papp ^d [nm/s]	P-gp efflux Ratio ^e		Microsomal stability CL _{int} ^f [(μl/min)/mg]		
		BACE1	HEK ^b	CatD			hER	rER	RLM	HLM	LipE ^g
21	Cl	0.021	0.19	1,100	53,000	28	2.8	2.9	<14	37	4.9
32	OMe	0.0075	0.052	1,200	160,000	25	2.0	3.1	<14	<14	5.4
27	Me	0.031	0.054	640	20,000	40	7.8	8.0	<14	16	5.1
28		0.0036	0.013	310	85,000	29	2.6	2.5	<14	<14	5.5
29		0.00057	0.0025	1,000	1,800,000	27	6.5	8.5	79	80	7.2
30		0.00062	0.0014	480	770,000	29	3.4	3.3	84	48	7.0

^aIC₅₀ values were averaged values determined by at least two independent experiments. ^bHuman embryonic kidney cells. ^cselectivity ratio [IC₅₀ CatD/IC₅₀ BACE1].

^dApparent permeability measured in parental LLC-PK1 cells. Values are an average of apical to basolateral (A to B) and basolateral to apical (B to A) velocities and are reported as nm/s. ^eEfflux measured in LLC-PK1 cells transfected with human MDR1 and are reported as a ratio of (B to A)/(A to B). ^fRat liver microsomal (RLM) and human liver microsomal (HLM) clearance reported as apparent intrinsic clearance with no correction for binding and not scaled. Compound concentration = 1 μM. Microsomal protein concentration = 0.25 mg/mL. ^gLipE = -log₁₀(BACE1 IC₅₀) - cLogP(calculated)

Table 4 Reduction of A β ₄₀ levels in CSF and brain in wild-type Sprague-Dawley rats and additional profiling

Cpd ^a	Aβ ₄₀ Reduction [%] ^b		Estimated EC _{50,unbound} [μM] ^c		C _{plasma,unbound} [μM] ^d	C _{CSF} [μM] ^e	Shift	pK _a
	CSF	Brain	CSF	Brain			Brain EC ₅₀ /Cell IC ₅₀	
1	74	65	0.011	0.017	0.032	0.06	0.81	5.6 ^f
28	66	52	0.012	0.021	0.022	0.02	1.5	NA ^g
29	58	25	0.011	0.030	0.015	0.005	12	NA ^g
30	62	41	0.0049	0.011	0.0078	0.003	7.9	6.1 ^h

^aCompounds were dosed orally 10 mg/kg as a solution (2% HMPC, 1% Tween80) to male Sprague-Dawley rats. n = 5 animals per group. ^bCSF and brain A β ₄₀ measured at t = 4 h. ^cEstimated unbound plasma EC₅₀ for CSF or brain effect from a single dose experiment at 4h timepoint or unbound plasma concentration corresponding to 50% A β ₄₀ in CSF or brain, respectively. ^dUnbound Plasma drug concentration measured at t = 4 h. ^eCSF drug concentration measured at t = 4 h. ^fexperimental pK_a determined by potentiometry at T = 25 °C. ^gNA = not available. ^hexperimental pK_a determined by UV spectrophotometry at T = 25 °C.

An indirect response model was used to model the PK-PD relationship which accounts for the formation and clearance of $A\beta_{40}$ in the CSF.⁶³ Using this model in vivo unbound plasma IC_{50} values for CSF and brain effect were generated (15 nM and 17 nM, respectively). These values were in good agreement with the estimated unbound plasma EC_{50} values obtained in the single dose, single time point PD study (5 nM and 11 nM, respectively).

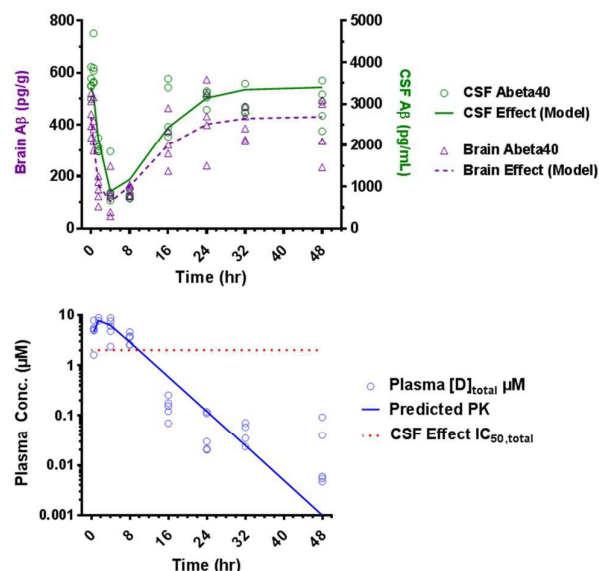


Fig 5. Time dependent $A\beta_{40}$ reduction in CSF and brain in rat after 30 mg/kg oral dose of **30** and total plasma concentrations of compound **30** measured in the same time-course study.

The pharmacokinetic (PK) profile of **30** was evaluated in rat and dog (Table 5). Consistent with the in vitro rat microsomal stability data, **30** showed moderate clearance in rat. Moderate clearance and similar V_{dss} was also maintained in dog. Taking into account the different protein binding of **30** in rat versus dog, unbound clearance was lower in dog ($Cl_{unbound} = 15.6$ L/h/kg) compared to rat ($Cl_{unbound} = 80$ L/h/kg). The bioavailability was calculated to be moderate in both species (%F = 30).

Table 5 Pharmacokinetic profiles and plasma protein binding of **30**

Species	iv ^a		po ^b			PPB F _u
	Cl [L/h/kg]	V _{dss} [L/kg]	C _{max} [μM]	t _{1/2} [h]	%F	
Rat	0.61	1.2	0.7	2.4	28	0.0076
Dog	0.36	1.3	0.7	4.5	30	0.023

^aRat: 2 mg/kg dose as a solution in DMSO; Dog: 1 mg/kg dose as a solution in 25% captisol/75% water at pH = 4; ^b5 mg/kg dose (rat) or 2 mg/kg dose (dog) as a solution in 1% Tween80/2% HMPC/97% water at pH = 2 (rat) or pH = 5 (dog).

A x-ray co-crystal structure of **30** in BACE1 overlaid with CatD protein is shown in Figure 6 (PDB 5I3W).^{64, 65} Every interaction of the BACE1 protein with the amino-oxazoline-warhead, the

3-aza-xanthene backbone and the P2' substituent is conserved compared to AOX-BACE1 inhibitors absent of a deep-P3 substituent. Figure 5 highlights the hydrogen-bonding between the NH of the amide and the backbone carbonyl of Gly230 as well as the near co-planarity of the amide linker between the 3-aza-AOX core and the 2-pyridyl. The picolinamide extends into the S3 sub-pocket and the chlorine in para-position engages in a repulsive steric interaction with the Asp318 resulting in the very high CatD selectivity of this compound. When tested against a panel of other aspartyl proteases, compound **30** showed high selectivity for BACE1 over Cathepsin E, pepsin and renin, but no selectivity over homologue BACE2.

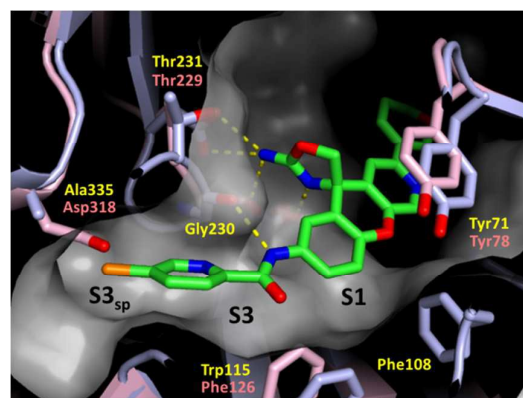


Fig 6. Co-crystal structure of human BACE1 (blue) + compound **30** (green, PDB 5I3W) overlaid with CatD (pink). Key residues are labeled in yellow for BACE1 and pink for CatD.

Compound **30** demonstrated a significant pharmacodynamic response and an acceptable PK profile in rat and dog. To further evaluate the likelihood for retinal toxicity of compound **30**, a 4-day repeat dose toxicology study was conducted in male Sprague Dawley rats.⁶⁶ Animals were administered daily oral doses of vehicle, 100, 300 and 900 mg/kg (n=3/dose level) of compound **30** for 4 days and necropsied 24 hours after the last dose. After the last dose, the mean exposure (area under the curve; AUC_{0-24}) was 985 $\mu\text{g}\cdot\text{h/mL}$ at 900 mg/kg. No test-article related increases in AFG in the RPE were observed at any dose level when evaluated by fluorescence microscopy.¹² Thus, at high multiples (127X) over the exposure necessary for 50% $A\beta_{40}$ reduction in the CSF ($AUC_{0-24} = 7.72$ $\mu\text{g}\cdot\text{h/mL}$ based on estimated total plasma drug concentration corresponding to 50% $A\beta_{40}$ reduction in the CSF $EC_{50,\text{total}} = 0.658$ nM) no microscopic changes in the retina were observed for **30** after 4 days. In contrast, we observed accumulation of AFG in the RPE after only 4 days after a daily oral 30 mg/kg dose of compound **1**, which corresponded to a 10X multiple.⁶⁷ During the evolution of AOX-BACE1 inhibitors great attention has been paid to the activity at the hERG cardiac ion channel.^{15, 56} Consequently, the cardiovascular (CV) effects of compound **30** were evaluated. Compound **30** was found to block hERG-mediated current in vitro ($IC_{50} = 0.9$ μM). The risk

of QTc prolongation was further assessed in an anesthetized dog cardiovascular model. Two male Beagle dogs were anesthetized and instrumented for cardiovascular monitoring before and after intravenous infusion of **30** at doses of 3.0, 7.5 and 25 mg/kg (30 min per dose). A blood sample was taken every 10 min at the end of each 30 min infusion to determine plasma drug concentration. After each dose of **30**, the average unbound plasma concentration was 0.11 μ M, 0.35 μ M and 0.85 μ M, respectively. These drug levels corresponded to unbound plasma concentrations of 9x, 25x and 59x fold over the unbound BACE IC₅₀ in the rat as determined by the indirect response model. Based on exposure-QTc prolongation response analysis (18 total PK-QT points; 9 per dog), plasma drug levels > 0.3 μ M (unbound) caused QTc interval prolongation (\geq 10% relative to baseline) in a concentration-dependent manner. We concluded, that the QTc prolongation observed for **30** in the dog was consistent with its hERG channel inhibition, and decided not to further pursue compound **30** due to the low cardiovascular safety margin.

Conclusions

In summary, a series of highly selective 2-aminooxazoline 3-aza-xanthene BACE1 inhibitors versus CatD were synthesized by installing substituents reaching into the S3 sub-pocket of the BACE1 protein. A combined structure- and property-based approach led to the identification of picolinamide-substituted 3-aza-AOX BACE1 inhibitors with suitable in vitro profiles, warranting further in vivo studies. Despite pushing the limits of physicochemical properties as they relate to CNS drug-likeness, the picolinamide-substituted 3-aza-AOX BACE1 inhibitors showed robust reduction of brain and CSF A β . The highly BACE1 over CatD selective compound **30** was further evaluated in a 4-day repeat toxicology study in rats and did not show any retinal effects, including AFG in the RPE, at doses up to 900 mg/kg. Despite our efforts culminating in the discovery of a picolinamide-substituted 3-aza-AOX-BACE1 inhibitor (**30**) with significantly greater selectivity over CatD, which appeared to have reduced the likelihood of retinal toxicity, a low safety margin for the elongation of the QTc interval in the dog cardiovascular model prevented the further assessment of compound **30**.

Acknowledgements

The authors thank Jennifer Allen for helpful discussions and editing of the manuscript, Kyung-Hyun Gahm, Wes Barnhart, Samuel Thomas, and Larry Miller for chiral separation; Patricia Lopez for scale-up of compound **30**; Alexander Long for purification of the BACE protein and Opas Nuanmanee for purification of the CatD protein; Steven Louie, Joel Esmay, Leeanne Zalameda and Yi Luo for performing in vitro screening of compounds; Paul H. Wen and Li Zhu for performing in vivo studies. The Advanced Light Source is supported by the U.S. Department of Energy under Contract No. DE-AC02-05CH11231.

Notes and references

1. E. Karran, M. Mercken and B. De Strooper, *Nature Reviews Drug Discovery*, 2011, **10**, 698-712.
2. K. M. Munro, A. Nash, M. Pignoni, S. F. Lichtenthaler and J. M. Gunnarsen, *Journal of Molecular Neuroscience*, 2016, **60**, 305-315.
3. T. Jonsson, J. K. Atwal, S. Steinberg, J. Snaedal, P. V. Jonsson, S. Bjornsson, H. Stefansson, P. Sulem, D. Gudbjartsson, J. Maloney, K. Hoyte, A. Gustafson, Y. Liu, Y. Lu, T. Bhangale, R. R. Graham, J. Huttenlocher, G. Bjornsdottir, O. A. Andreassen, E. G. Joensson, A. Palotie, T. W. Behrens, O. T. Magnusson, A. Kong, U. Thorsteinsdottir, R. J. Watts and K. Stefansson, *Nature (London, United Kingdom)*, 2012, **488**, 96-99.
4. J. Yuan, S. Venkatraman, Y. Zheng, B. M. McKeever, L. W. Dillard and S. B. Singh, *Journal of Medicinal Chemistry*, 2013, **56**, 4156-4180.
5. D. Oehrich, H. Prokopcova and H. J. M. Gijzen, *Bioorganic & Medicinal Chemistry Letters*, 2014, **24**, 2033-2045.
6. A. K. Ghosh and H. L. Osswald, *Chemical Society Reviews*, 2014, **43**, 6765-6813.
7. Y. Lu, D. Riddell, E. Hajos-Korcsok, K. Bales, K. M. Wood, C. E. Nolan, A. E. Robshaw, L. Zhang, L. Leung, S. L. Becker, E. Tseng, J. Barricklow, E. H. Miller, S. Osgood, B. T. O'Neill, M. A. Brodney, D. S. Johnson and M. Pettersson, *Journal of Pharmacology and Experimental Therapeutics*, 2012, **342**, 366-375.
8. P. C. May, R. A. Dean, S. L. Lowe, F. Martenyi, S. M. Sheehan, L. N. Boggs, S. A. Monk, B. M. Mathes, D. J. Mergott, B. M. Watson, S. L. Stout, D. E. Timm, E. S. LaBell, C. R. Gonzales, M. Nakano, S. S. Jhee, M. Yen, L. Ereshefsky, T. D. Lindstrom, D. O. Calligaro, P. J. Cocke, D. G. Hall, S. Friedrich, M. Citron and J. E. Audia, *Journal of Neuroscience*, 2011, **31**, 16507-16516.
9. R. Vassar, *Alzheimer's Research & Therapy*, 2014, **6**, 89/81-89/14, 14 pp.
10. C. Sheridan, *Nature Biotechnology*, 2015, **33**, 115-116.
11. E. Kennedy Matthew, X. Chen, A. Hodgson Robert, A. Hyde Lynn, R. Kuvelkar, M. Parker Eric, W. Stamford Andrew, N. Cumming Jared, W. Li, D. Scott Jack, K. Cox, F. Dockendorf Marissa, J. Kleijn Huub, H. Mei, A. Stone Julie, M. Egan, L. Ereshefsky, S. Jhee, A. Mattson Britta, J. Palcza, M. Tanen, D. Troyer Matthew, L. Tseng Jack and S. Forman Mark, *Science translational medicine*, 2016, **8**, 363ra150.
12. M. R. Fielden, J. Werner, J. A. Jamison, A. Coppi, D. Hickman, R. T. Dunn, II, E. Trueblood, L. Zhou, C. A. Afshari and R. Lightfoot-Dunn, *Toxicologic Pathology*, 2015, **43**, 581-592.
13. T. A. Dineen, K. Chen, A. C. Cheng, K. Derakhchan, O. Epstein, J. Esmay, D. Hickman, C. E. Kreiman, I. E. Marx, R. C. Wahl, P. H. Wen, M. M. Weiss, D. A. Whittington, S. Wood, R. T. Fremeau, R. D. White and V. F. Patel, *Journal of Medicinal Chemistry*, 2014, **57**, 9811-9831.
14. S. Khoh-Reiter, S. A. Sokolowski, B. Jessen, M. Evans, D. Dalvie and S. Lu, *Toxicological Sciences*, 2015, **145**, 383-395.
15. J. J. Chen, Q. Liu, C. Yuan, V. Gore, P. Lopez, V. Ma, A. Amegadzie, W. Qian, T. C. Judd, A. E. Minatti, J. Brown, Y. Cheng, M. Xue, W. Zhong, T. A. Dineen, O. Epstein, J. Human, C. Kreiman, I. Marx, M. M. Weiss, S. A. Hitchcock,

ARTICLE

MedChemComm

- T. S. Powers, K. Chen, P. H. Wen, D. A. Whittington, A. C. Cheng, M. D. Bartberger, D. Hickman, J. A. Werner, H. M. Vargas, N. E. Everds, S. L. Vonderfecht, R. T. Dunn, II, S. Wood, R. T. Freneau, Jr., R. D. White and V. F. Patel, *Bioorganic & Medicinal Chemistry Letters*, 2015, **25**, 767-774.
16. A. M. Zuhl, C. E. Nolan, M. A. Brodney, S. Niessen, K. Atchison, C. Houle, D. A. Karanian, C. Ambroise, J. W. Brulet, E. M. Beck, S. D. Doran, B. T. O'Neill, C. W. am Ende, C. Chang, K. F. Geoghegan, G. M. West, J. C. Judkins, X. Hou, D. R. Riddell and D. S. Johnson, *Nature Communications*, 2016, **7**, 13042.
 17. P. C. May, B. A. Willis, S. L. Lowe, R. A. Dean, S. A. Monk, P. J. Cocke, J. E. Audia, L. N. Boggs, A. R. Borders, R. A. Brier, D. O. Calligaro, T. A. Day, L. Ereshefsky, J. A. Erickso, H. Gevorkyan, C. R. Gonzales, D. E. James, S. S. Jhee, S. F. Komjathy, L. Li, T. D. Lindstrom, B. M. Mathe, F. Martenyi, S. M. Sheehan, S. L. Stout, D. E. Timm, G. M. Vaught, B. M. Watson, L. L. Winneroski, Z. Yang and D. J. Mergott, *Journal of Neuroscience*, 2015, **35**, 1199-1210, 1112 pp.
 18. C. R. Butler, M. A. Brodney, E. M. Beck, G. Barreiro, C. E. Nolan, F. Pan, F. Vajdos, K. Parris, A. H. Varghese, C. J. Helal, R. Lira, S. D. Doran, D. R. Riddell, L. M. Buzon, J. K. Dutra, L. A. Martinez-Alsina, K. Ogilvie, J. C. Murray, J. M. Young, K. Atchison, A. Robshaw, C. Gonzales, J. Wang, Y. Zhang and B. T. O'Neill, *Journal of Medicinal Chemistry*, 2015, **58**, 2678-2702.
 19. U. Neumann, H. Rueeger, R. Machauer, S. J. Veenstra, R. M. Lueoend, M. Tintelnot-Blomley, G. Laue, K. Beltz, B. Vogg, P. Schmid, W. Frieauff, D. R. Shimshek, M. Staufenbiel and L. H. Jacobson, *Molecular Neurodegeneration*, 2015, **10**, 44/41-44/15.
 20. R. Steinfeld, K. Reinhardt, K. Schreiber, M. Hillebrand, R. Kraetzer, W. Brueck, P. Saftig and J. Gaertner, *American Journal of Human Genetics*, 2006, **78**, 988-998.
 21. Standard deviations for the in vitro CatD enzymatic assay can be found in the supporting information.
 22. E. T. Baldwin, T. N. Bhat, S. Gulnik, M. V. Hosur, R. C. Sowder, R. E. Cachau, J. Collins, A. M. Silva and J. W. Erickson, *Proceedings of the National Academy of Sciences of the United States of America*, 1993, **90**, 6796-6800.
 23. Y. Cheng, J. Brown, T. C. Judd, P. Lopez, W. Qian, T. S. Powers, J. J. Chen, M. D. Bartberger, K. Chen, R. T. Dunn, O. Epstein, R. T. Freneau, S. Harried, D. Hickman, S. A. Hitchcock, Y. Luo, A. E. Minatti, V. F. Patel, H. M. Vargas, R. C. Wahl, M. M. Weiss, P. H. Wen, R. D. White, D. A. Whittington, X. M. Zheng and S. Wood, *ACS Medicinal Chemistry Letters*, 2015, **6**, 210-215.
 24. S. Yonezawa, T. Takahashi, X. J. Wang, R. N. S. Wong, J. A. Hartsuck and J. Tang, *Journal of Biological Chemistry*, 1988, **263**, 16504-16511.
 25. N. P. Birch and Y. P. Loh, *Nucleic Acids Research*, 1990, **18**, 6445-6446.
 26. In this publication, substituents on the aminooxazoline xanthene core were named in accordance with the space they occupy in the catalytic domain of the BACE1 enzyme as it was determined by X-ray cocrystal structure of previous AOX BACE1 inhibitors with BACE1 protein. For example, the substituents binding in the S3 region of the enzyme are named P3 substituents, those binding in the S3 sp pocket are named P3 sp or deep P3 substituents, those binding in the S2' pocket are named P2' substituents.
 27. S. J. Stachel, C. A. Coburn, D. Rush, K. L. G. Jones, H. Zhu, H. Rajapakse, S. L. Graham, A. Simon, M. Katharine Holloway, T. J. Allison, S. K. Munshi, A. S. Espeseth, P. Zuck, D. Colussi, A. Wolfe, B. L. Pietrak, M.-T. Lai and J. P. Vacca, *Bioorganic & Medicinal Chemistry Letters*, 2009, **19**, 2977-2980.
 28. H. A. Rajapakse, P. G. Nantermet, H. G. Selnick, J. C. Barrow, G. B. McGaughey, S. Munshi, S. R. Lindsley, M. B. Young, P. L. Ngo, M. Katherine Holloway, M.-T. Lai, A. S. Espeseth, X.-P. Shi, D. Colussi, B. Pietrak, M.-C. Crouthamel, K. Tugusheva, Q. Huang, M. Xu, A. J. Simon, L. Kuo, D. J. Hazuda, S. Graham and J. P. Vacca, *Bioorganic & Medicinal Chemistry Letters*, 2010, **20**, 1885-1889.
 29. C. R. Ellis and J. Shen, *Journal of the American Chemical Society*, 2015, **137**, 9543-9546.
 30. C. R. Ellis, C.-C. Tsai, X. Hou and J. Shen, *Journal of Physical Chemistry Letters*, 2016, **7**, 944-949.
 31. T. J. Woltering, W. Wostl, H. Hilpert, M. Rogers-Evans, E. Pinard, A. Mayweg, M. Gobel, D. W. Banner, J. Benz, M. Travagli, M. Pollastrini, G. Marconi, E. Gabellieri, W. Guba, H. Mauser, M. Andreini, H. Jacobsen, E. Power and R. Narquizian, *Bioorganic & Medicinal Chemistry Letters*, 2013, **23**, 4239-4243.
 32. H. Hilpert, W. Guba, T. J. Woltering, W. Wostl, E. Pinard, H. Mauser, A. V. Mayweg, M. Rogers-Evans, R. Humm, D. Krummenacher, T. Muser, C. Schnider, H. Jacobsen, L. Ozmen, A. Bergadano, D. W. Banner, R. Hochstrasser, A. Kuglstatler, P. David-Pierson, H. Fischer, A. Polara and R. Narquizian, *Journal of Medicinal Chemistry*, 2013, **56**, 3980-3995.
 33. N. Anderson and J. Borlak, *FEBS Letters*, 2006, **580**, 5533-5540.
 34. D. A. Price, J. Blagg, L. Jones, N. Greene and T. Wager, *Expert Opinion on Drug Metabolism & Toxicology*, 2009, **5**, 921-931.
 35. J.-U. Peters, J. Hert, C. Bissantz, A. Hillebrecht, G. Gerebtzoff, S. Bendels, F. Tillier, J. Migeon, H. Fischer, W. Guba and M. Kansy, *Drug discovery today*, 2012, **17**, 325-335.
 36. S. A. Hitchcock and L. D. Pennington, *Journal of Medicinal Chemistry*, 2006, **49**, 7559-7583.
 37. T. T. Wager, R. Y. Chandrasekaran, X. Hou, M. D. Troutman, P. R. Verhoest, A. Villalobos and Y. Will, *ACS Chemical Neuroscience*, 2010, **1**, 420-434.
 38. T. T. Wager, X. Hou, P. R. Verhoest and A. Villalobos, *ACS Chemical Neuroscience*, 2010, **1**, 435-449.
 39. J. N. Cumming, E. M. Smith, L. Wang, J. Misiaszek, J. Durkin, J. Pan, U. Iserloh, Y. Wu, Z. Zhu, C. Strickland, J. Voigt, X. Chen, M. E. Kennedy, R. Kuvelkar, L. A. Hyde, K. Cox, L. Favreau, M. F. Czarniecki, W. J. Greenlee, B. A. McKittrick, E. M. Parker and A. W. Stamford, *Bioorganic & Medicinal Chemistry Letters*, 2012, **22**, 2444-2449.
 40. A. W. Stamford, J. D. Scott, S. W. Li, S. Babu, D. Tadesse, R. Hunter, Y. Wu, J. Misiaszek, J. N. Cumming, E. J. Gilbert, C. Huang, B. A. McKittrick, L. Hong, T. Guo, Z. Zhu, C. Strickland, P. Orth, J. H. Voigt, M. E. Kennedy, X. Chen, R. Kuvelkar, R. Hodgson, L. A. Hyde, K. Cox, L. Favreau, E. M. Parker and W. J. Greenlee, *ACS Medicinal Chemistry Letters*, 2012, **3**, 897-902.

41. B.-M. Swahn, K. Kolmodin, S. Karlstroem, S. von Berg, P. Soederman, J. Holenz, S. Berg, J. Lindstroem, M. Sundstroem, D. Turek, J. Kihlstroem, C. Slivo, L. Andersson, D. Pyring, D. Rotticci, L. Oehberg, A. Kers, K. Bogar, M. Bergh, L.-L. Olsson, J. Janson, S. Eketjaell, B. Georgievskia, F. Jeppsson and J. Faeltling, *Journal of Medicinal Chemistry*, 2012, **55**, 9346-9361.
42. S. Eketjaell, J. Janson, F. Jeppsson, A. Svanhagen, K. Kolmodin, S. Gustavsson, A.-C. Radesaeter, K. Eliason, S. Briem, P. Appelkvist, C. Niva, A.-L. Berg, S. Karlstroem, B.-M. Swahn and J. Faeltling, *Journal of Neuroscience*, 2013, **33**, 10075-10084.
43. S. Eketjaell, J. Janson, K. Kaspersson, A. Bogstedt, F. Jeppsson, J. Faeltling, S. B. Haeberlein, A. R. Kugler, R. C. Alexander, G. Cebers and P. Ho, *Journal of Alzheimer's Disease*, 2016, **50**, 1109-1123.
44. K. W. Hunt, A. W. Cook, R. J. Watts, C. T. Clark, G. Vigers, D. Smith, A. T. Metcalf, I. W. Gunawardana, M. Burkard, A. A. Cox, M. K. Geck Do, D. Dutcher, A. A. Thomas, S. Rana, N. C. Kallan, R. K. DeLisle, J. P. Rizzi, K. Regal, D. Sammond, R. Groneberg, M. Siu, H. Purkey, J. P. Lyssikatos, A. Marlow, X. Liu and T. P. Tang, *Journal of Medicinal Chemistry*, 2013, **56**, 3379-3403.
45. Y. Gravenfors, J. Viklund, J. Blid, T. Ginman, S. Karlstroem, J. Kihlstroem, K. Kolmodin, J. Lindstroem, S. von Berg, F. von Kieseritzky, K. Bogar, C. Slivo, B.-M. Swahn, L.-L. Olsson, P. Johansson, S. Eketjaell, J. Faeltling, F. Jeppsson, K. Stroemberg, J. Janson and F. Rahm, *Journal of Medicinal Chemistry*, 2012, **55**, 9297-9311.
46. Y.-J. Wu, J. Guernon, R. Rajamani, J. H. Toyn, M. K. Ahlijanian, C. F. Albright, J. Muckelbauer, C. Chang, D. Camac, J. E. Macor and L. A. Thompson, *Bioorganic & Medicinal Chemistry Letters*, 2016, DOI: 10.1016/j.bmcl.2016.10.055, Ahead of Print.
47. M. Ciordia, L. Perez-Benito, F. Delgado, A. A. Trabanco and G. Tresadern, *Journal of Chemical Information and Modeling*, 2016, **56**, 1856-1871.
48. M. P. Huestis, W. Liu, M. Volgraf, H. E. Purkey, C. Yu, W. Wang, D. Smith, G. Vigers, D. Dutcher, K. W. Hunt and M. Siu, *Tetrahedron Letters*, 2013, **54**, 5802-5807.
49. Y.-J. Wu, J. Guernon, F. Yang, L. Snyder, J. Shi, A. McClure, R. Rajamani, H. Park, A. Ng, H. Lewis, C. Y. Chang, D. Camac, J. H. Toyn, M. K. Ahlijanian, C. F. Albright, J. E. Macor and L. A. Thompson, *ACS Medicinal Chemistry Letters*, 2016, **7**, 271-276.
50. F. J. R. Rombouts, G. Tresadern, O. Delgado, C. Martinez-Lamenca, M. Van Gool, A. Garcia-Molina, S. A. Alonso de Diego, D. Oehlich, H. Prokopcova, J. M. Alonso, N. Austin, H. Borghys, S. Van Brandt, M. Surkyn, M. De Cleyn, A. Vos, R. Alexander, G. Macdonald, D. Moechars, H. Gijssen and A. A. Trabanco, *Journal of Medicinal Chemistry*, 2015, **58**, 8216-8235.
51. G. Tresadern, F. Delgado, O. Delgado, H. Gijssen, G. J. Macdonald, D. Moechars, F. Rombouts, R. Alexander, J. Spurlino, M. Van Gool, J. A. Vega and A. A. Trabanco, *Bioorganic & Medicinal Chemistry Letters*, 2011, **21**, 7255-7260.
52. N. Kobayashi, K. Ueda, N. Itoh, S. Suzuki, G. Sakaguchi, A. Kato, A. Yukimasa, A. Hori, Y. Koriyama, H. Haraguchi, K. Yasui, Y. Kanda, Shionogi & Co., Ltd. WO2007049532, 2007.
53. J. D. Scott, S. W. Li, A. P. J. Brunskill, X. Chen, K. Cox, J. N. Cumming, M. Forman, E. J. Gilbert, R. A. Hodgson, L. A. Hyde, Q. Jiang, U. Iserloh, I. Kazakevich, R. Kuvelkar, H. Mei, J. Meredith, J. Misiaszek, P. Orth, L. M. Rossiter, M. Slater, J. Stone, C. O. Strickland, J. H. Voigt, G. Wang, H. Wang, Y. Wu, W. J. Greenlee, E. M. Parker, M. E. Kennedy and A. W. Stamford, *Journal of Medicinal Chemistry*, 2016, **59**, 10435-10450.
54. A. S. Guram, X. Wang, E. E. Bunel, M. M. Faul, R. D. Larsen and M. J. Martinelli, *Journal of Organic Chemistry*, 2007, **72**, 5104-5112.
55. Y. Chen, R. White, A. Amegadzie, J. Brown, A. C. Cheng, E. F. Dimauro, T. Dineen, V. K. Gore, J. B. Human, T. Judd, C. Kreiman, Q. Liu, P. Lopez, V. V. Ma, I. Marx, A. E. Minatti, H. N. Nguyen, N. A. Paras, V. F. Patel, W. Qian, M. Weiss, Q. Xue, X. M. Zheng, W. Zhong, Amgen Inc. WO2011115938, 2011.
56. O. Epstein, M. C. Bryan, A. C. Cheng, K. Derakhchan, T. A. Dineen, D. Hickman, Z. Hua, J. B. Human, C. Kreiman, I. E. Marx, M. M. Weiss, R. C. Wahl, P. H. Wen, D. A. Whittington, S. Wood, X. M. Zheng, R. T. Fremeau, Jr., R. D. White and V. F. Patel, *Journal of Medicinal Chemistry*, 2014, **57**, 9796-9810.
57. D.-Y. Lee and J. F. Hartwig, *Organic Letters*, 2005, **7**, 1169-1172.
58. J. Andersen, U. Madsen, F. Bjorkling and X. Liang, *Synlett*, 2005, DOI: 10.1055/s-2005-872248, 2209-2213.
59. Z. J. Kaminski, P. Paneth and J. Rudzinski, *Journal of Organic Chemistry*, 1998, **63**, 4248-4255.
60. A. Falchi, G. Giacomelli, A. Porcheddu and M. Taddei, *Synlett*, 2000, DOI: 10.1055/s-2000-6490, 275-277.
61. As suggested in a previous publication (ref 19), attention should not be limited to achieving a high numerical CatD/BACE1 selectivity ratio but also to the absolute CatD IC50 value.
62. An estimate of unbound EC50 for Ab lowering was calculated from a single dose, single time point (4 h) experiment assuming a standard sigmoid dose response (Hill slope of 1). This approach was initially validated by comparing EC50 values from a dose response experiment to the single dose, single time point estimate of unbound EC50. Subsequently, estimated EC50s have been shown to be a good approximation of the IC50 determined from a time course experiment using an indirect response PK/PD model.
63. M. A. Felmler, M. E. Morris and D. E. Mager, *Methods in Molecular Biology (New York, NY, United States)*, 2012, **929**, 583-600.
64. A x-ray co-crystal structure of compound 30 in BACE1 protein has previously been published in a different context (PDB ID 5I3W).
65. J. B. Jordan, D. A. Whittington, M. D. Bartberger, E. A. Sickmier, K. Chen, Ryan D. White, Y. Cheng and T. Judd, *Journal of Medicinal Chemistry*, 2016, **59**, 3732-3749.
66. Male Sprague Dawley rats (*Rattus norvegicus*, Crl:CD®(SD); Charles River Laboratories; 10 weeks of age) were group-housed at an AAALAC, International-accredited facility. Animals were cared for in accordance with the Guide for the Care and Use of Laboratory Animals, 8th Edition. All research protocols were reviewed and approved by the Amgen Institutional

ARTICLE

MedChemComm

Animal Care and Use Committee. Rats were housed in an individual ventilated caging system on an irradiated corncob bedding (Envigo Teklad 7097). Lighting in animal holding rooms was maintained on 12:12 hr light:dark cycle, and the ambient temperature and humidity range was at 68°F to 79°F and 30% to 70%, respectively. Animals had ad libitum access to irradiated pelleted feed (Envigo Teklad Global Rodent Diet; soy protein free extruded 2020X) and reverse-osmosis chlorinated (0.3 to 0.5 ppm) water via an automatic watering system. Cages were changed weekly inside an engineered cage changing station.

67. unpublished results.

Development of 2-Aminooxazoline 3-Azaxanthene β -Amyloid Cleaving Enzyme (BACE) Inhibitors with Improved Selectivity Against Cathepsin D

Jonathan D. Low, Michael D. Bartberger, Kui Chen, Yuan Cheng, Mark R. Fielden, Vijay Gore, Dean Hickman, Qingyian Liu, E. Allen Sickmier, Hugo M. Vargas, Jonathan Werner, Ryan D. White, Douglas A. Whittington, Stephen Wood, Ana E. Minatti,*

We report the discovery of an orally efficacious 3-aza-aminooxazoline-BACE1 inhibitor with 1,800,000X fold selectivity against CatD and no retinal effects in an early screening rat toxicology study.

